BRL

REPORT No. 886

ENIAC Computation of
Two-Dimensional Supersonic Nozzles

NATHAN GERBER

BALLISTIC RESEARCH LABORATORIES

ABERDEEN PROVING GROUND, MARYLAND

b. "Initial distribution has been made of this report in accordance with the distribution list contained herein. Additonal distribution without recourse to the Ordnance Office may be made to United States military organizations, and to such of their contractors as they certify to be cleared to receive this report and to need it in the furtherance of a military contract."

BALLISTIC RESEARCH LABORATORIES

REPORT NO. 886

DECEMBER 1953

ENIAC COMPUTATION OF TWO-DIMENSIONAL SUPERSONIC NOZZLES

Nathan Gerber

ABERDEEN PROVING GROUND, MARYLAND

SYMBOLS

x, y	rectangular position coordinates
$\bar{q}$	velocity vector
u, v	rectangular velocity components
q, θ	polar coordinates of velocity
q_o	speed of radial flow on initial circular arc
a	local speed of sound
γ	ratio of specific heats ($=1.4$ for air)
M	Mach number ($=q/a$)
θ_o	inclination of bounding ray of radial flow
$\mathcal{K}$	curvature of nozzle
α, β	characteristic coordinates (α varies on the patching characteristics)
$H \equiv a^2 - u^2 \quad L \equiv a^2 - v^2$	
$K \equiv -uv \quad R \equiv a(q^2 - a^2)^{1/2}$	
λ, μ	direction cosines of straight line ($\alpha = $ const.) simple wave characteristic
r	length of $\alpha = $ const. simple wave characteristic
ρ	density
ξ, η	x, y along characteristic which patches the transition and simple wave regions
s	arc length along transition section of nozzle
$\Delta\theta$	parameter governing rate of growth of curvature of transition section

2

BALLISTIC RESEARCH LABORATORIES

REPORT NO. 886

NGerber/lr
Aberdeen Proving Ground, Md.
December 1953

ENIAC COMPUTATION OF TWO-DIMENSIONAL SUPERSONIC NOZZLES

ABSTRACT

A procedure based on the method of characteristics is described in detail for computing two-dimensional supersonic nozzles with continuous curvature everywhere. The results of ENIAC calculations of a series of nozzles by this method are summarized briefly.

SECTION I

INTRODUCTION

This report will describe a method of determining two-dimensional supersonic nozzles on the basis of plane isentropic flow of a perfect gas. The computational procedure is based on the method of characteristics (ref. [1]).
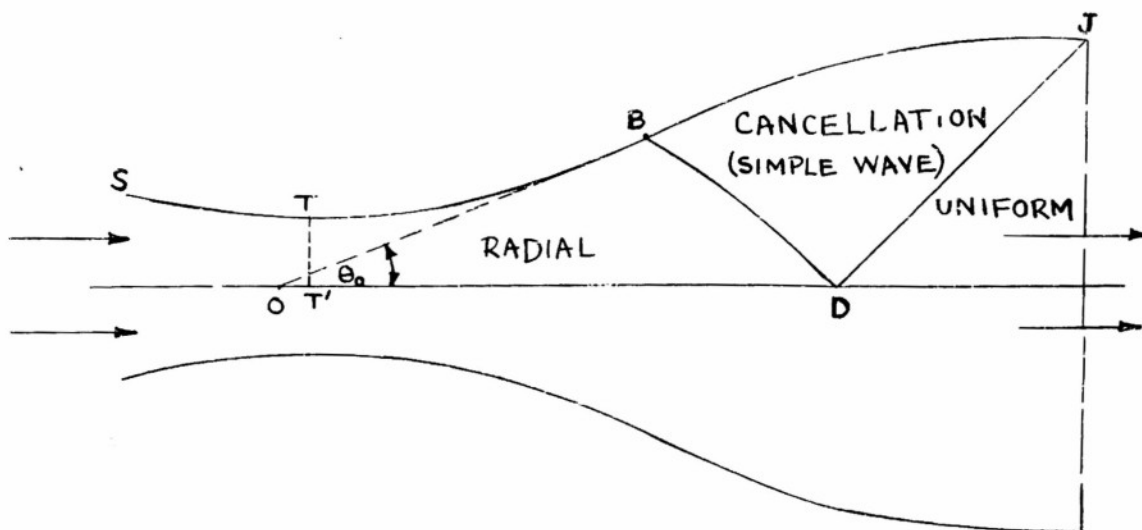

Fig 1.1

The procedure commonly used for designing these nozzles (ref. [2]) is to patch a "simple wave" onto an assumed initial radial flow to obtain the "cancellation" region which leads to uniform flow. These several regions are indicated in Fig 1.1, which shows a representative two-dimensional nozzle. (Because of symmetry we need only refer to the upper half of the diagram.) The radial flow originates from a two-dimensional source at point O, the ray OB being tangent to the contour TBJ at the "inflection" point B. BD and DJ are characteristics (or Mach lines)*. The problem is the determination of BJ.

Nozzles designed in the above manner will, in general, have discontinuous wall curvature at points B and J (Fig 1.1). While this condition is permissible for fixed throat tunnels, it is unsatisfactory for flexible throat tunnels, the walls of which must have continuous curvature everywhere. The process used in the calculations described in this report avoids

---

* See, e.g., pp. 259 - 286 of ref. [3] for discussion of simple waves and Mach lines.

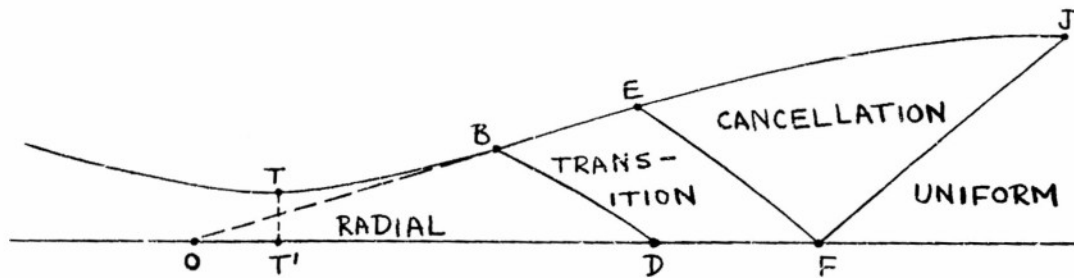this trouble by inserting between the radial flow and the simple

Fig 1.2

wave a transition section (BDFE in Fig 1.2) the wall curvature of which
varies continuously from zero to the value at the beginning of the can-
cellation section. The transition section can be fitted in many ways.
The particular method used here is described in Section II by eqn. (2.6)
and its accompanying discussion.

A series of calculations described in Section IV were performed on
the ENIAC to provide design data for the 13" x 15" flexible nozzle wind
tunnel (No. 1) now under construction for the Supersonic Wind Tunnels
Branch of the Exterior Ballistics Laboratory. These shapes were selected
from a three-parameter (q_o, θ_o, $\Delta\theta$) family of nozzles. The particular
choices of parameters were guided by factors such as physical limitations
on tunnel lengths and permissible plate curvatures. The object was to
get a continuously varying family of nozzles from which could be obtained
reasonable shapes of curves ("jack displacement" vs. Mach number) for the
design of cams governing automatic settings of the jacks which hold the
wall in place.

To obtain the final family of eighteen nozzles required about one
hundred and ten trials at about forty-five minutes per case. Clearly
computations on this scale would never have been undertaken by hand.

EQUATIONS AND BOUNDARY CONDITIONS

The equations describing the two-dimensional flows are (ref. [1], p.12)

$$H \ \partial u/\partial x + K \ (\partial u/\partial y + \partial v/\partial x) + L \ \partial v/\partial y = 0 \Bigg\}$$
$$\partial v/\partial x - \partial u/\partial y = 0 \qquad (2.1)$$

where $H \equiv a^2-u^2$, $K \equiv -uv$, $L \equiv a^2-v^2$.

The flow field is divided into four regions (Fig 2.1): I -- radial flow, II -- general two-dimensional flow, III -- simple wave, and IV -- uniform flow. These regions are separated by the characteristic curves
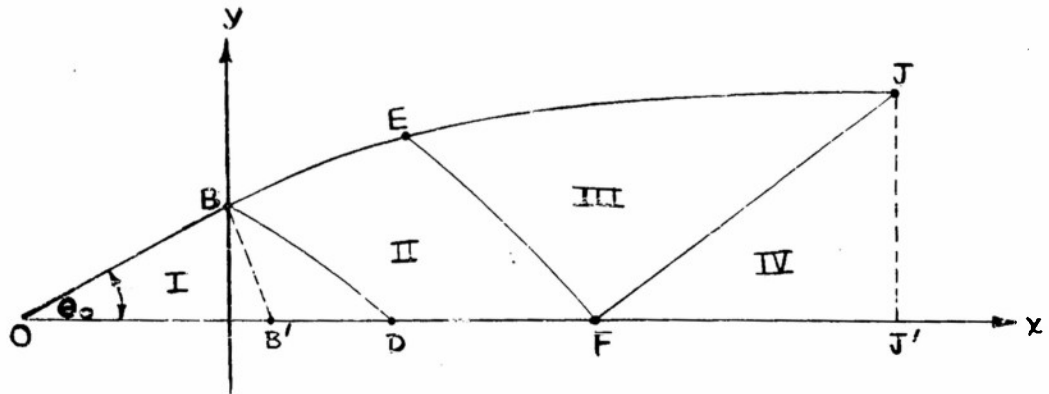

Fig. 2.1

BD, EF, and FJ; BB' is a circular arc.

The boundary conditions are

a) v=0 when y=0;

that is, the air flows along the center line of a cross-section of the nozzle.

b) $v/u = f'(x)$ along a contour $f(x)$, which is to be determined as part of the solution to the problem. This contour is subject to the following conditions: $f'(x) = \tan \theta_o$, $f''(x) = 0$ at point B; $f'(x) = 0$ at point J; $f(x)$ has continuous curvature $\mathcal{K}(x)$ everywhere between B and J.

We first establish the coordinate system. The origin is determined so that $x_B = 0$, $y_B = 1$ (Fig 2.2).
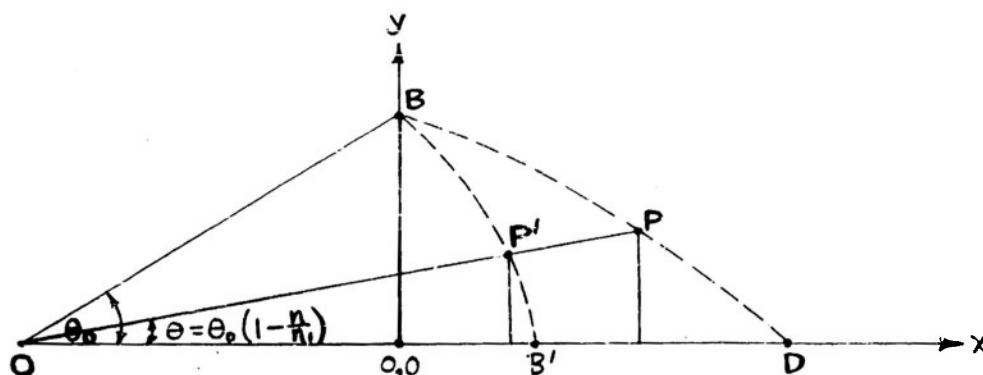

Fig. 2.2

The initial information at our disposal is the radial flow, with speed q_0 on BB'. Since the streamlines coincide with the rays from point O, θ measures the inclination of both. The angle θ_0 is divided into n_1 intervals of magnitute $\delta\theta = \theta_0/n_1$, where n_1 is an integer.

Clearly, on equally spaced points on BB'

$$x(n) = \csc\theta_0 \cos(\theta_0 - n\theta_0/n_1) - \cot\theta_0$$

$$y(n) = \csc\theta_0 \sin(\theta_0 - n\theta_0/n_1)$$

$$u(n) = q_0 \cos(\theta_0 - n\theta_0/n_1)$$

$$v(n) = q_0 \sin(\theta_0 - n\theta_0/n_1)$$

(2.2)

where $n = 0, 1, 2, \ldots, n_1$. Accordingly, $n = 0$ for point B and increases along the curve up to n_1 at point B'.

We designate α as the variable along BD, the Mach line patching together the regions I and II. In the solution of problems by characteristics the choice of characteristic parameter along certain bounding Mach lines is arbitrary (see ref. [1], p. 21). Thus we are able to

8

choose $\alpha = n$ along BD; that is, α will vary continuously with θ from zero at B to $n_1 = \alpha_1$ at D, and at any point P (Fig. 2.2), where $\theta = \theta_o(1-n/n_1)$, α will be equal to n.

Since the hodograph of the plane characteristic BD is a Prandtl-Busemann epicycloid, the velocity distribution on BD is described by

$$\theta_o - \theta = f(M) - f(M_o), \text{ where}$$

$$f(M) \equiv \cos^{-1}(1/M) - \sqrt{(\gamma+1)/(\gamma-1)} \; \tan^{-1}\left(\sqrt{M^2-1} \; \sqrt{(\gamma-1)/(\gamma+1)}\right),$$

(see ref. [4], p. 26) and $M(q) \equiv \sqrt{2q^2/\left[(\gamma-1)(1-q^2)\right]}$; also $M_o = M(q_o)$.

(2.3)

To determine the curve BD, consider the streamline OP (Fig. 2.2)

$$\overline{OP}/\overline{OP}' = y_P/y_{P'}$$

$$\overline{OP}' = \csc \theta_o$$

Thus $\ell_P \equiv \overline{OP} = (y_P/y_{P'}) \csc \theta_o$.

P and P' may be taken as two points on a two-dimensional nozzle surface. Then (ref. [5], p. 34)

$$y_P/y_{P'} = (A_P/A^*)/(A_{P'}/A^*)$$

A/A* is the ratio of the cross-sectional area at any point in a two-dimensional nozzle to that at the throat of the nozzle (according to one-dimensional theory, M=1 at the throat) and is a function of q.

$$A/A^* = (1/M)\left[\left\{2+(\gamma-1)M^2\right\}/(\gamma+1)\right]^{(\gamma+1)/(2\gamma-2)}$$

Since $q_{P'}$ ($=q_o$) and $q_P(\alpha)$ are known, $\ell_P(\alpha)$ can be determined.

Let $\theta = \theta_o(1-n/n_1) = \theta_o(1-\alpha/\alpha_1) = \theta(\alpha)$ at point P.

Then
$$x(\alpha) = \ell_P \cos(1-\alpha/\alpha_1)\theta_o - \cot\theta_o$$
$$y(\alpha) = \ell_P \sin(1-\alpha/\alpha_1)\theta_o$$
$$u(\alpha) = q(\alpha)\cos(1-\alpha/\alpha_1)\theta_o$$
$$v(\alpha) = q(\alpha)\sin(1-\alpha/\alpha_1)\theta_o$$

(2.4)

9

Consequently $x(\alpha)$, $y(\alpha)$, $u(\alpha)$, $v(\alpha)$ are determined at $\alpha_1 + 1$ points on BD.

We transform to the characteristic (α, β) plane to determine the flow in region II. The characteristic equations are (ref. [1]),

$$
\left.
\begin{aligned}
(K-R)\, y_\alpha - L x_\alpha &= 0 \\
H\, y_\beta - (K-R) x_\beta &= 0 \\
H\, u_\alpha + (K-R) v_\alpha &= 0 \\
(K-R) u_\beta + L v_\beta &= 0
\end{aligned}
\right\}
\qquad (2.5)
$$

$(\bar{y}_\alpha \equiv \partial y / \partial \alpha,\; y_\beta \equiv \partial y / \partial \beta,\; \text{etc.})$

where $R = \sqrt{K^2 - HL}$. Fig. 2.3 shows the map of region II in the characteristic plane. The two bounding streamlines BE and DF map into the lines $\beta = \alpha$
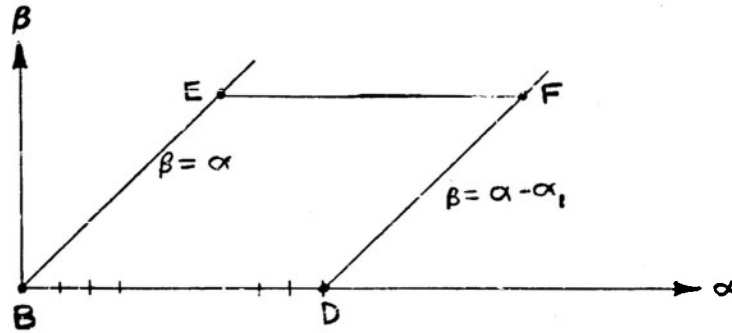
Fig. 2.3

and $\beta = \alpha - \alpha_1$ respectively ($d\beta / d\alpha = 1$ on them).

We arbitrarily demand that the inclination of the nozzle on BE be of the form

$$
\theta = \theta_o - \alpha^2 \Delta\theta \qquad (2.6)
$$

where $\Delta\theta > 0$ is a prescribed constant. The curvature on BE is

$$
\mathcal{K}_i = d\theta/ds = -2\alpha \Delta\theta / s_\alpha .
$$

At B, $\alpha = 0$, so $\mathcal{K}_i = 0$. Thus the condition of zero curvature of the nozzle at point B is satisfied. More generally $\theta = \theta_o - \alpha^2 g(\alpha)$, where $g(\alpha)$ is an arbitrary function of α, satisfies this condition.

Since

$$
\partial s/\partial \alpha = (\partial x/\partial \alpha)\sqrt{1 + (dy/dx)^2} = (\partial x/\partial \alpha)\sqrt{1 + \tan^2(\theta_o - \alpha^2 \Delta\theta)},
$$

the curvature is

$$\mathcal{K}_i = -2\alpha\,\Delta\theta\Big/\Big[(\partial x/\partial\alpha)\ \sqrt{1 + \tan^2\,(\theta_o - \alpha^2\,\Delta\theta)}\Big] \qquad (2.7)$$

The flow in region III is a simple wave; that is, the velocity is constant along the characteristics α = constant, which are straight lines. Consequently the points on EJ, the remainder of the nozzle, are simply functions of α. In particular, $\theta_J = \theta\,(\alpha_1) = 0$, and q_F is the speed of the final uniform flow.
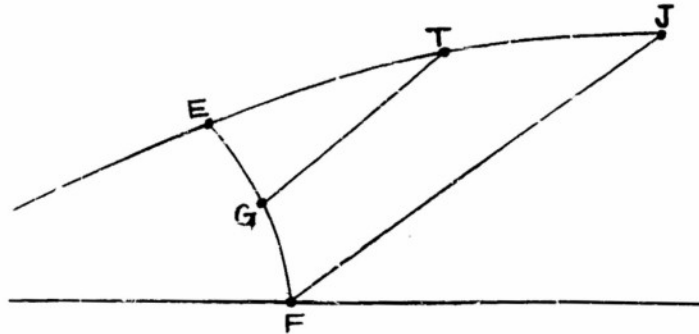

Fig. 2.4

We wish to locate a point, say T, on EJ (Fig. 2.4) which corresponds to the point G on EF. Let $x = \xi$, $y = \eta$ on EF. Then $x_G = \xi\,(\alpha)$, $y_G = \eta\,(\alpha)$. The slope of GT is

$$m(\alpha) = \Big[(\partial y/\partial\beta)\ /\ (\partial x/\partial\beta)\Big]_G = (K-R)\ /\ H \qquad \text{(from eqn. (2.5))}.$$

The unit vector tangent to GT is (λ,μ), where

$$\lambda = -H\Big/\sqrt{H^2 + (K-R)^2}\,,\ \ \mu = -(K-R)\sqrt{H^2 + (K-R)^2}. \qquad (2.8)$$

Then on EJ

$$\left.\begin{aligned}
x(\alpha) &= \xi\,(\alpha) + \lambda\,(\alpha)\,r\,(\alpha) = x_T\\
y(\alpha) &= \eta\,(\alpha) + \mu\,(\alpha)\,r\,(\alpha) = y_T\\
u(\alpha) &= \qquad\qquad\qquad\ = u_T\\
v(\alpha) &= \qquad\qquad\qquad\ = v_T
\end{aligned}\right\} \qquad\qquad r\,(\alpha) = \overline{GT} \qquad\qquad (2.9)$$

We find $r\,(\alpha)$ essentially from the equation of continuity by equating

11

the mass per second of air flowing across GT to the mass per second across EG.

Q_{GT} = mass/sec. across GT = $\rho(\alpha)\left[u(\alpha)\mu(\alpha) - v(\alpha)\lambda(\alpha)\right]r(\alpha)$.

$(u\mu - v\lambda)$ is the scalar product of the vector $\bar{q} = (u,v)$ and the vector $(\mu, -\lambda)$, a unit vector normal to the line GT. It is also the component of the velocity normal to the characteristic GT, which is equal to $a(\alpha)$, the speed of sound.

From ref. [1], p. 12, $\rho = \rho_0(1 - q^2)^{1/(\gamma-1)}$ (ρ_0 being constant for the flows considered here; h=1), and $a^2 = (\gamma-1)(1-q^2)/2$. Hence

$$Q_{GT} = \rho_0(1 - q^2)^{1/(\gamma-1)} a(\alpha)\, r(\alpha).$$

A unit vector, normal to the curve EF is $(-\eta_\alpha/\sqrt{\xi_\alpha^2 + \eta_\alpha^2},$ $\xi_\alpha/\sqrt{\xi_\alpha^2 + \eta_\alpha^2}$); and Q_{EG} = mass/sec. across EG = $\int_0^{s_{EG}}\left[\rho(v\xi_\alpha - u\eta_\alpha)/\sqrt{\xi_\alpha^2 + \eta_\alpha^2}\right]ds$.

But $ds/d\alpha = \sqrt{\xi_\alpha^2 + \eta_\alpha^2}$; so

$$Q_{EG} = \rho_0\int_{\alpha_E}^{\alpha}(1-q^2)^{1/(\gamma-1)}(v\xi_\alpha - u\eta_\alpha)\,d\alpha.$$

Equating Q_{EG} and Q_{GT}, we get (taking $\gamma = 1.4$)

$$r(\alpha) = \left[\int_{\alpha_E}^{\alpha}(1-q^2)^{2.5}(v\xi_\alpha - u\eta_\alpha)\,d\alpha\right]\Big/\left[a(1-q^2)^{2.5}\right]$$

According to eqn. (2.5) $\eta_\alpha = \left[L/(K-R)\right]\xi_\alpha = (K+R)\xi_\alpha/H$; so finally

$$r(\alpha) = \left\{\int_{\alpha_E}^{\alpha}(1-q^2)^{2.5}\left[v - (K+R)u/H\right]\xi_\alpha\,d\alpha\right\}\Big/\left\{a(\alpha)\left[1-q^2(\alpha)\right]^{2.5}\right\}$$

(2.10)

Along EJ $dy/dx = v(\alpha)/u(\alpha)$, $d^2y/dx^2 = \left[d(v/u)/d\alpha\right]/(dx/d\alpha)$. The curvature is

$$K = \left[d^2y/dx^2\right]\Big/\left[1+(dy/dx)^2\right]^{3/2} = (u/q)^3\left[d(v/u)/d\alpha\right]/(dx/d\alpha).$$

(2.11)

At point E, where $r = 0$, we note that (by eqn. (2.9))

$$(dx/d\alpha)\big]_E = (d\xi/d\alpha)\big]_E + \lambda(dr/d\alpha)\big]_E$$

(2.12)

12

By eqn. (2.10)

$$(1-q^2)^{1/(\gamma-1)} \; a \; dr/d\alpha \Big]_E = (1-q^2)^{1/(\gamma-1)} \left\{ v \, d\xi/d\alpha \Big]_E - u \, d\eta/d\alpha \Big]_E \right\}$$

This leads to the relation

$$dr/d\alpha \Big]_E = \left\{ -q^2\lambda \; / \; (a^2 - u^2) \right\} \; d\xi/d\alpha \Big]_E \;,$$

which upon substitution into eqn. (2.12) leads to

$$dx/d\alpha \Big]_E = - \left\{ 2\lambda u \sqrt{q^2 - a^2} \; \Big/ \; (a^2 - u^2) \right\} d\xi/d\alpha \Big]_E \qquad (2.13)$$

By eqn. (2.5), $\lambda \; du/d\alpha + \mu \; dv/d\alpha = 0$, and

$$d(v/u) \; / \; d\alpha = (uv_\alpha - vu_\alpha)/u^2 = - (\sqrt{q^2 - a^2} \; / \; \mu u^2) \; u_\alpha \;.$$

Substituting this relation and eqn. (2.13) into eqn. (2.11) we finally obtain

$$\mathcal{K}_E = \left[(a^2 - u^2) \; /(2q^3\lambda\mu) \right] (u_\alpha/\xi_\alpha)_E \qquad (2.14)$$

Actually, the length of the transition section is not known a priori. In the computation at each point on BJ (Fig. 2.1) both $\mathcal{K}_i$ (eqn. (2.7)) and $\mathcal{K}_E$ (eqn. (2.14)) are computed. When a point E where $\mathcal{K}_i = \mathcal{K}_E$ is found, generally by interpolation, the characteristic EF is constructed and the cancellation section thus started. To achieve a desired design Mach number at the uniform flow region several trials must generally be made with various initial q_0's on BB'.

SECTION III

COMPUTATIONAL PROCEDURES

The initial data for determining the flow on BD (Fig. 2.1) are available on IBM output cards as a result of a previous ENIAC computation of Prandtl-Meyer flow. (See eqn. (2.3).) A/A^* and q_0 have been tabulated at .05 degree intervals of $\omega \equiv \theta +$ const. The input deck for a computation is extracted from this main deck by selecting first the card with $q = q_0$ (on which ω is, say, ω_0), then those cards with $\omega = \omega_0 + \delta \theta$, $\omega = \omega_0 + 2\delta\theta, \ldots, \omega = \omega_0 + n_1\delta\theta = \omega_0 + \theta_0$. Eqns. (2.4) then yield x,y,u,v at a_1+1 equally spaced points on BD ($\beta=0$) in the characteristic plane (Fig. 2.3).

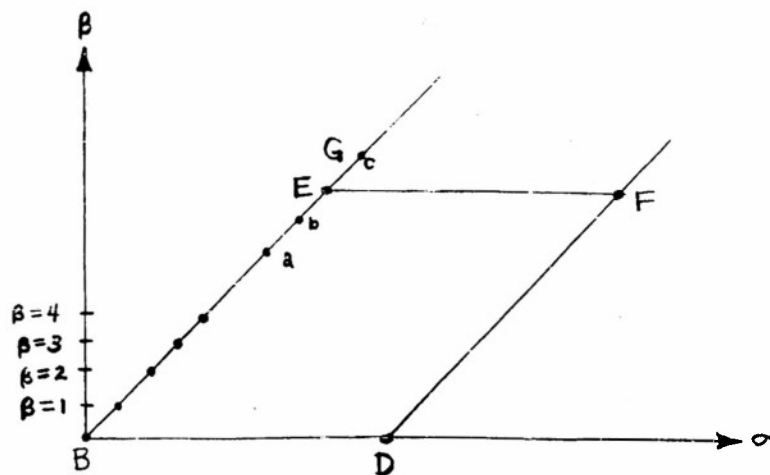For region II there are three computational routines: the stream process for points on

Fig. 3.1

DF (Fig. 3.1), the nozzle process for points on BE, and the general process for all other points. The second order iterative method described in detail in ref. [1] is used to solve the differential

14

equations numerically[*]. The partial derivatives are replaced by differences, so that for a point P (Fig. 3.2), with information known
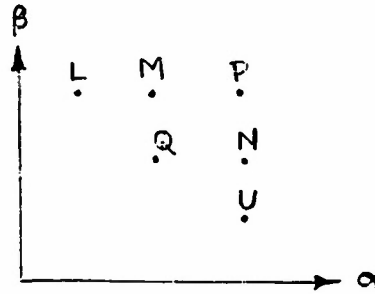

Fig. 3.2

at points L and U, eqns. (2.5) become

$$
\begin{aligned}
(K\text{-}R)_{\cancel{Q}M}(y_P\text{-}y_L) - L_{\cancel{Q}M}(x_P\text{-}x_L) &= 0 \\
H_{\cancel{Q}N}(y_P\text{-}y_U) - (K\text{-}R)_{\cancel{Q}N}(x_P\text{-}x_U) &= 0 \\
H_{\cancel{Q}M}(u_P\text{-}u_L) + (K\text{-}R)_{\cancel{Q}M}(v_P\text{-}v_L) &= 0 \\
(K\text{-}R)_{\cancel{Q}N}(u_P\text{-}u_U) + L_{\cancel{Q}N}(v_P\text{-}v_U) &= 0
\end{aligned}
\right\} \tag{3.1}
$$

The notation $H_{\cancel{Q}M}$ means that H is evaluated first at Q, then in the second iteration at M. $H_Q=(H_U+H_L)/2$; $H_M=(H_P+H_L)/2$; $H_N=(H_P+H_U)/2$, where H_P is computed from u_P, v_P determined in the first iteration. This notation applies similarly to all other coefficients.

The solution (general process) to eqns. (3.1) is

$$
\begin{aligned}
x_P &= (K\text{-}R)_{\cancel{Q}M}\left\{H_{\cancel{Q}N}\, y_U - (K\text{-}R)_{\cancel{Q}N}\, x_U\right\}/D - \\
&\quad H_{\cancel{Q}N}\left\{(K\text{-}R)_{\cancel{Q}M}\, y_L - L_{\cancel{Q}M}\, x_L\right\}/D \\
y_P &= L_{\cancel{Q}M}\left\{H_{\cancel{Q}N}\, y_U - (K\text{-}R)_{\cancel{Q}N}\, x_U\right\}/D - \\
&\quad (K\text{-}R)_{\cancel{Q}N}\left\{(K\text{-}R)_{\cancel{Q}M}\, y_L - L_{\cancel{Q}M}\, x_L\right\}/D \\
u_P &= L_{\cancel{Q}N}\left\{H_{\cancel{Q}M}\, u_L + (K\text{-}R)_{\cancel{Q}M}\, v_L\right\}/\Delta - \\
&\quad (K\text{-}R)_{\cancel{Q}M}\left\{(K\text{-}R)_{\cancel{Q}N}\, u_U + L_{\cancel{Q}N}\, v_U\right\}/\Delta \\
v_P &= H_{\cancel{Q}M}\left\{(K\text{-}R)_{\cancel{Q}N}\, u_U + L_{\cancel{Q}N}\, v_U\right\}/\Delta - \\
&\quad (K\text{-}R)_{\cancel{Q}N}\left\{H_{\cancel{Q}M}\, u_L + (K\text{-}R)_{\cancel{Q}M}\, v_L\right\}/\Delta
\end{aligned}
\right\} \tag{3.2}
$$

---

[*]It should be remarked that the ENIAC coding used was actually adapted (to save coding time) from existing axisymmetric flow coding by suppressing $a^2 v/y$ terms.

15

where

$$D = L_{\emptyset M} \, H_{\emptyset N} - (K-R)_{\emptyset M} \, (K-R)_{\emptyset N} \quad \text{and}$$

$$\triangle = H_{\emptyset M} \, L_{\emptyset N} - (K-R)_{\emptyset N} \, (K-R)_{\emptyset M}$$

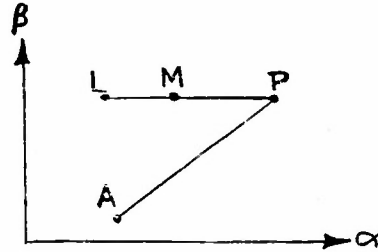Similarly, the stream process computation (DF in Fig. 3.1) for point P in Fig. 3.3 is

Fig. 3.3

$$\left. \begin{aligned} x_P = x_L &= \left\{ (K-R)\big/ L \right\}_{LM} y_L \,, & y_P &= 0 \\ u_P = u_L &+ \left\{ (K-R)\big/ H \right\}_{LM} v_L \,, & v_P &= 0 \end{aligned} \right\} \tag{3.3}$$

The equations used for the nozzle process (BE in Fig. 3.1) are

$$\left. \begin{aligned} H v_\beta &- (K-R) \, x_\beta = 0 \\ (K-R) u_\beta &+ L \, v_\beta = 0 \\ dy/dx &= \tan(\theta_o - \alpha^2 \Delta\theta) \\ v &= u \tan(\theta_o - \alpha^2 \Delta\theta) \end{aligned} \right\} \tag{3.4}$$
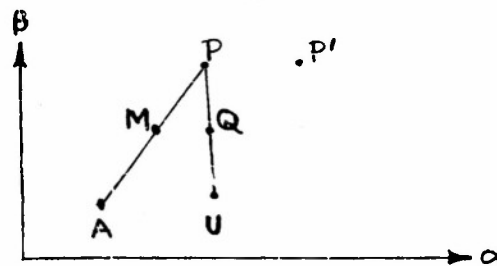

Fig. 3.4

16

In difference form they are (see Fig. 3.4)

$$\left\{H/(K-R)\right\}_{\not{Q}} (y_P - y_U) - (x_P - x_U) = 0$$

$$(u_P - u_U) + \left\{L/(K-R)\right\}_{\not{Q}} (v_P - v_U) = 0$$

$$(y_P - y_A)/(x_P - x_A) - \tan_M(\theta_o - \alpha^2 \Delta\theta) = 0 \tag{3.5}$$

$$u_P \tan(\theta_o - \alpha_P^2 \Delta\theta) - v_P = 0$$

where $\tan_M(\theta_o - \alpha^2 \Delta\theta) = (1/2)\left[\tan(\theta_o - \alpha_A^2 \Delta\theta) + \tan(\theta_o - \alpha_P^2 \Delta\theta)\right]$.

The solution to eqns. (3.5), which locates the nozzle points, is

$$x_P = (1/A)\left\{\left[H/(K-R)\right]_{\not{Q}} y_U - x_U\right\} +$$

$$(1/A)\left\{\left[H/(K-R)\right]_{\not{Q}}\left[-y_A + x_A \tan_M(\theta_o - \alpha^2 \Delta\theta)\right]\right\}$$

$$y_P = (1/A)\left\{-y_A + x_A \tan_M(\theta_o - \alpha^2 \Delta\theta)\right\} -$$

$$(1/A)\left\{-\left[H/(K-R)\right]_{\not{Q}} y_U + x_U\right\} \tan_M(\theta_o - \alpha^2 \Delta\theta) \tag{3.6}$$

$$u_P = (1/B)\left\{\left[L/(K-R)\right]_{\not{Q}} v_U + u_U\right\}$$

$$v_P = (1/B)\left\{\left[L/(K-R)\right]_{\not{Q}} v_U + u_U\right\} \tan(\theta_o - \alpha_P^2 \Delta\theta)$$

where

$$A = \left\{H/(K-R)\right\}_{\not{Q}} \tan_M(\theta_o - \alpha^2 \Delta\theta) - 1$$

$$B = \left\{L/(K-R)\right\}_{\not{Q}} \tan(\theta_o - \alpha_P^2 \Delta\theta) + 1$$

The flow is computed at $\alpha_1 + 1$ equally spaced points on $\beta = 1$, then on $\beta = 2$, $\beta = 3$, and so on.

The partial derivatives in the curvature expression eqns. (2.7) and (2.14) are approximated by linear difference quotients. Thus (see Fig. 3.4)

$$(\partial x/\partial\alpha)_P \cong (x_{P'} - x_P)/(\alpha_{P'} - \alpha_P); \quad (\partial u/\partial\alpha)_P \cong (u_{P'} - u_P)/(\alpha_{P'} - \alpha_P) .$$

17

For every nozzle point K_i and $K_s = \left[(a^2-u^2)u_\alpha\right]\Big/\left[2q^3\lambda\mu\,x_\alpha\right]$
are computed, and $\delta \equiv K_i - K_s$ is recorded. δ varies monotonically along
the nozzle; and when it changes sign at some point G (Fig. 3.1), we
know that the point E, where the transition region curvature equals that
for a simple wave, has been reached and passed. Using the information
at G and the two preceding nozzle points, we determine by three point
interpolation the variables for $\delta = 0$; namely, x_E, y_E, u_E, v_E, α_E, β_E.

The characteristic $\beta = \beta_E$ (EF in Fig. 3.1), on which $x = \xi(\alpha)$, $y = \eta(\alpha)$
is then computed in the same manner as the preceding β = const. character-
istics. The Mach number at F is the final exit Mach number.

The remainder of the flow is the cancellation region and is computed
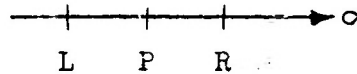from eqns. (2.9) and (2.10).

In evaluating the integrand in eqn. (2.10)

Fig. 3.5

we approximate the derivatives $\xi_\alpha(\alpha)$ by central differences (i.e.,
$\xi_\alpha(\alpha) \cong \left[\xi(\alpha+1) - \xi(\alpha-1)\right]\Big/\left[2\alpha\right]$) for all points but the first
two and the last two. For the first two points $\partial\xi/\partial\alpha\big]_P \cong \left[(\xi_R-\xi_P)/(\alpha_R-\alpha_P)\right]$
(see Fig. 3.5), and for the last two points $\partial\xi/\partial\alpha\big]_P \simeq \left[(\xi_P-\xi_L)/(\alpha_P-\alpha_L)\right]$.

We approximate the integral in eqn. (2.10), which we write as
$$T(\alpha) = \int_{\alpha_E}^{\alpha} J(\alpha)\,d\alpha$$, by Simpson's formula for all points but the first
two and the last one: namely,
$$T(\alpha) \cong T(\alpha-2) + \left\{\left[J(\alpha-2) + 4J(\alpha-1) + J(\alpha)\right]/3\right\}.$$
$T(\alpha = \alpha_E) = 0$ for the first point. $T_P \cong T_L + \left[(J_L + J_P)(\alpha_P - \alpha_L)/2\right]$
(see Fig. 3.5) for the second and last points.

Finally, for the wind tunnel designer's convenience, the coordinates
of the nozzle points were transformed so that the exit point F has the
coordinates $X_F = 0$, $Y_F = E$, an assigned constant. This calculation places
all the nozzles on a scale based on a fixed height of the wind tunnel test
section. The transformation was accomplished by
$$\left.\begin{aligned} X &= (E/y_F)(x_F - x)\\ Y &= (E/y_F)\,y \end{aligned}\right\} \qquad (3.7)$$

SECTION IV

SUMMARY OF COMPUTATIONS

Fig. 4.1 indicates the flow regions and Mach lines of a typical nozzle calculation.

The nozzles computed for the Wind Tunnels Branch are summarized graphically in Fig. 4.2. Contours were computed at intervals of .25 for exit Mach numbers ranging from 1.25 to 5.5. The actual numerical computations are available in the files of the Data Reduction Unit of the Supersonic Wind Tunnels Branch, Exterior Ballistics Laboratory.

The designs for the remaining sections of the wind tunnel walls ("subsonic" and "expansion" sections - ST and TB in Fig. 1.1) were obtained empirically after the ENIAC data became available. Boundary layer corrections were included in all the jack settings.

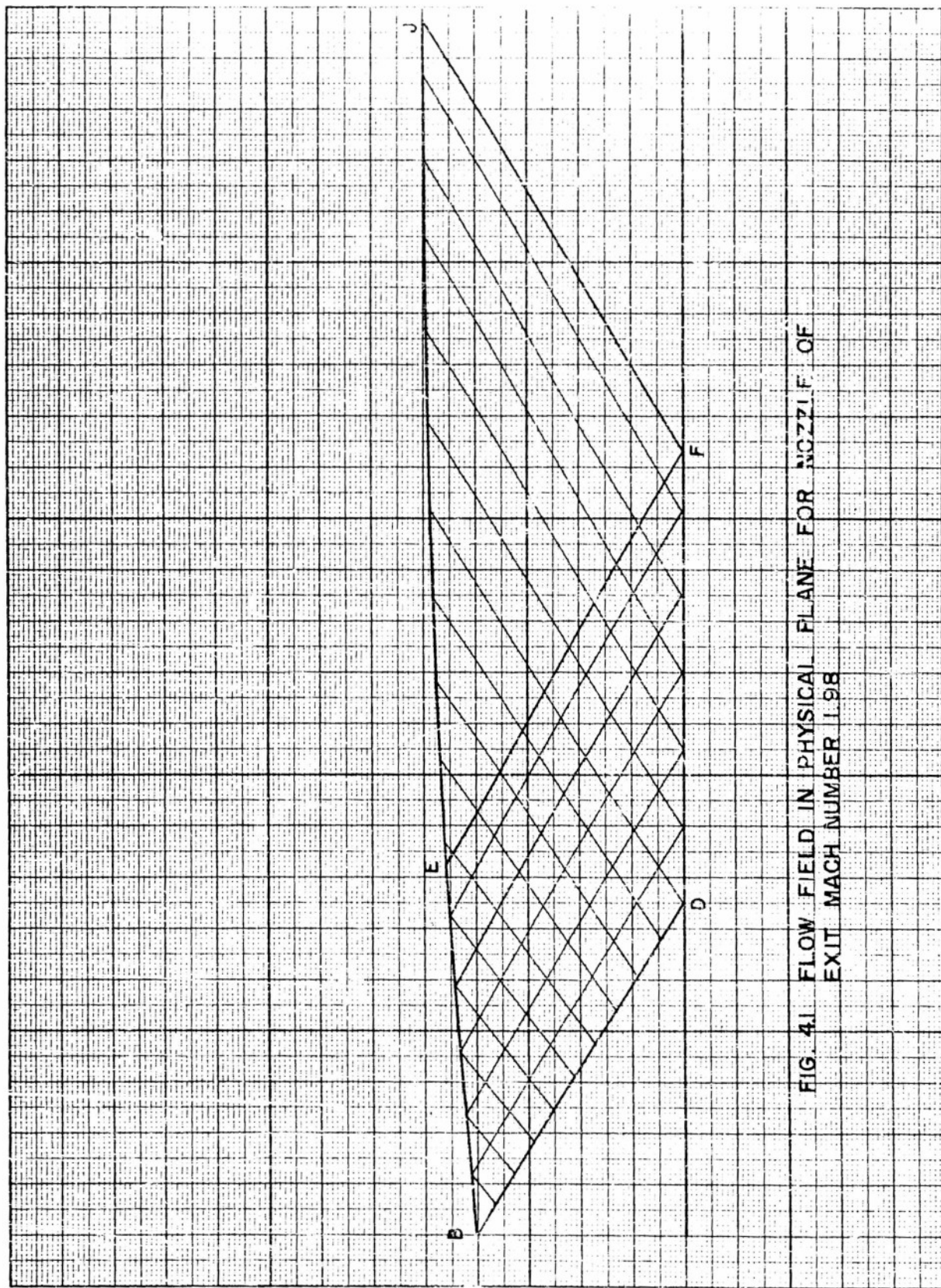## ACKNOWLEDGEMENTS

Nathan Gerber

NATHAN GERBER

FIG. 4.1 FLOW FIELD IN PHYSICAL PLANE FOR NOZZLE OF
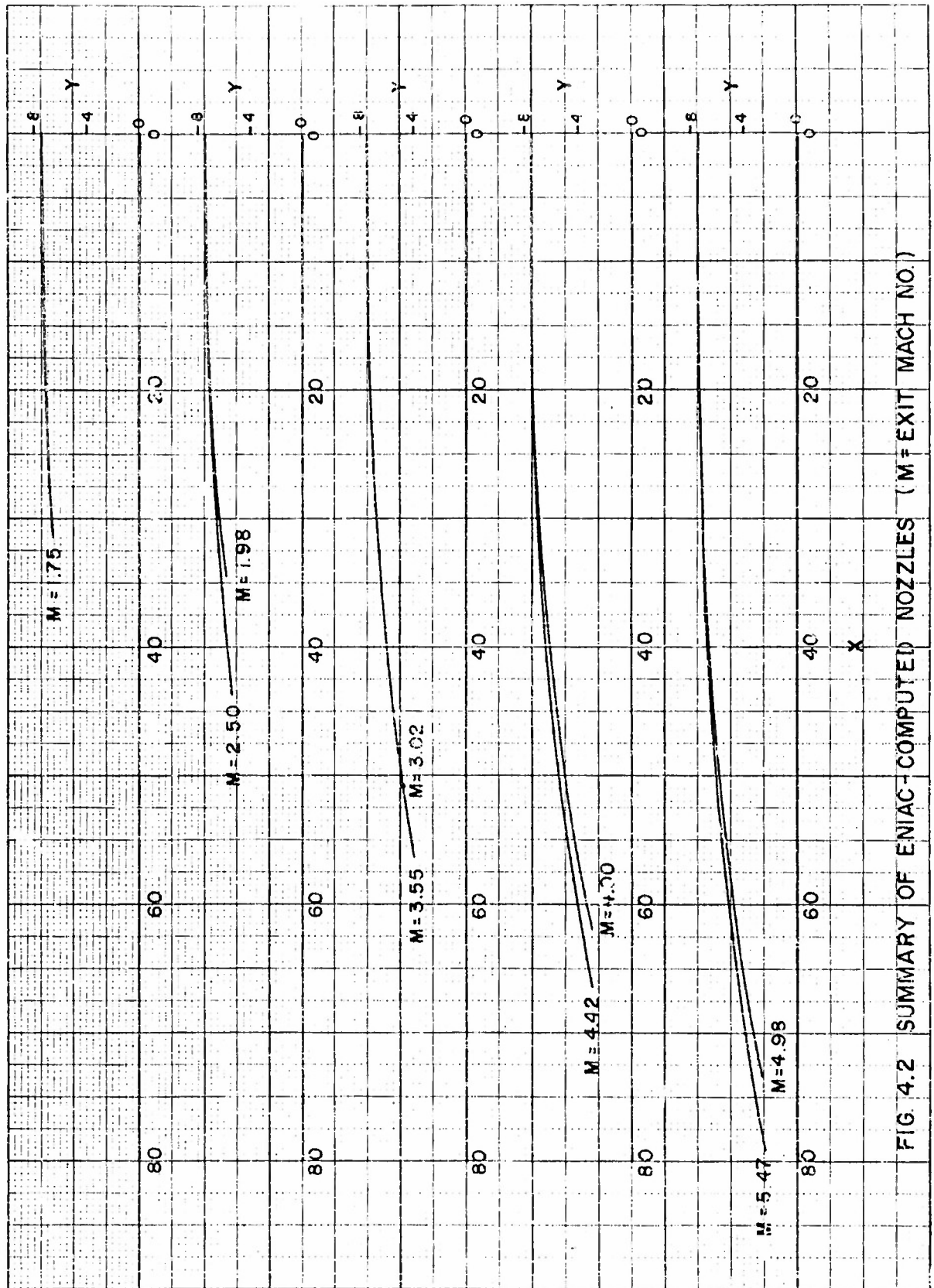EXIT MACH NUMBER 1.98

FIG. 4.2 SUMMARY OF ENIAC-COMPUTED NOZZLES (M=EXIT MACH NO.)

REFERENCES

1. Clippinger, R. F. and Gerber, N. : Supersonic Flow over Bodies of Revolution (with Special Reference to High Speed Computing). BRL Report 719. May 1950.

2. Foelsch, Kuno: A New Method of Designing Two Dimensional Laval Nozzles for a Parallel and Uniform Jet. North American Aviation Report NA-46-235. March 1946.

3. Courant, R. and Friedricks, K. O. : Supersonic Flow and Shockwaves. Interscience Publishers, 1948.

4. Ferri, Antonio: Aerodynamics of Supersonic Flows. The Mac Millan Co., (New York), 1949.

5. Liepmann, H. W. and Puckett, A. E.: Introduction to Aerodynamics of a Compressible Fluid. John Wiley and Sons Inc., 1947.

DISTRIBUTION LIST

No. of Copies	Organization	No. of Copies	Organization
6	Chief of Ordnance Department of the Army Washington 25, D. C. Attn: ORDTB - Bal Sec	1	Commanding Officer & Director David W. Taylor Model Basin Washington 7, D. C. Attn: Aerodynamics Laboratory
10	British - ORDTB for distribution	1	Director Air University Library Maxwell Air Force Base, Alabama
4	Canadian Joint Staff - ORDTB for distribution	4	Commander Air Research & Development Command P. O. Box 1395 Baltimore 3, Maryland Attn: Deputy for Development
4	Chief, Bureau of Ordnance Department of the Navy Washington 25, D. C. Attn: Re3		
2	ASTIA Reference Center Library of Congress Washington 25, D. C.	5	Director Armed Services Technical Information Agency Documents Service Center Knott Building Dayton 2, Ohio Attn: DSC - SA
2	Commander Naval Proving Ground Dahlgren, Virginia		
2	Commander Naval Ordnance Laboratory White Oak Silver Spring 19, Maryland	3	Commanding General Redstone Arsenal Huntsville, Alabama
1	Commander Naval Ordnance Test Station Inyokern P. O. China Lake, California Attn: Technical Library	1	Commanding General Arnold Engineering Development Center Tullahoma, Tennessee Attn: Deputy Chief of Staff, R&D
1	Superintendent Naval Postgraduate School Monterey, California	5	Director National Advisory Committee for Aeronautics 1724 F Street, N. W. Washington 25, D. C. Attn: Division Research Information
1	Commander Naval Air Development Center Johnsville, Pennsylvania		
2	Commander Naval Air Missile Test Center Point Mugu, California	2	Director National Advisory Committee for Aeronautics Ames Laboratory Moffett Field, California Attn: Dr. A. C. Charters Mr. H. J. Allen

DISTRIBUTION LIST

No. of Copies	Organization	No. of Copies	Organization
1	Professor George Carrier Division of Applied Sciences Harvard University Cambridge 38, Massachusetts	1	Wright-Aeronautical Corp. Wood-Ridge, New Jersey Attn: Sales Department (Government)
1	Professor Francis H. Clauser Department of Aeronautics Johns Hopkins University Baltimore 18, Maryland	2	Applied Physics Laboratory 8621 Georgia Avenue Silver Spring, Maryland Attn: Mr. George L. Seielstad
1	Professor Clark B. Millikan Director, Guggenheim Aeronautical Laboratory 1500 Normandy Drive California Institute of Technology Pasadena 4, California	1	Cornell Aeronautical Laboratory Inc. Buffalo, New York Attn: Miss Elma T. Evans Librarian
1	Dr. A. E. Puckett Hughes Aircraft Company Florence Avenue at Teal Street Culver City, California	1	M. W. Kellogg Company Foot of Danforth Avenue Jersey City 3, New Jersey Attn: Mr. Robert A. Miller
1	Dr. L. H. Thomas Watson Scientific Computing Laboratory 612 West 116th Street New York 27, New York	1	The Firestone Tire & Rubber Co. Defense Research Division Akron 17, Ohio Attn: Peter J. Ginge
1	North Carolina State College Raleigh, North Carolina Attn: Professor J. W. Cell	1	General Electric Co. Project HERMES Schenectady, New York Attn: Mr. J. C. Hoffman
1	Norman Bridge Laboratory of Physics California Institute of Technology Pasadena, California Attn: Dr. Leverett Davis, Jr.	1	United Aircraft Corp. Research Department East Hartford 8, Connecticut Attn: Mr. Robert C. Sale
1	University of Virginia Department of Mathematics Charlottesville, Virginia Attn: Professor Edward J. McShane	1	Aerophysics Development Corp. P. O. Box 657 Pacific Palisades, California Attn: Dr. William Bellay
1	A. D. Little, Inc. Cambridge 42, Massachusetts Attn: Dr. C. S. Keevil	1	University of Southern California Engineering Center Los Angeles 7, California Attn: Mr. H. R. Saffell

DISTRIBUTION LIST

No. of Copies	Organization
1	Consolidated Vultee Aircraft Corp. Ordnance Aerophysics Laboratory Daingerfield, Texas Attn: Mr. J. E. Arnold
1	California Institute of Technology Pasadena, California Attn: Library
2	Massachusetts Institute of Technology Cambridge 39, Massachusetts Attn: Guided Missiles Library, Room 22-001
2	California Institute of Technology Jet Propulsion Laboratory Pasadena, California Attn: Mr. Irl E. Newlan, Reports Group
1	University of Michigan Willow Run Research Center Willow Run Airport Ypsilanti, Michigan Attn: Mr. J. E. Corey